Intrinsic control of DRG sensory neuron diversification by Pten

Alejandra Fernandez[1‡], Nick Sarn[2], Charis Eng[2,3,4], Kevin M. Wright[1,‡]

[1]Vollum Institute, Oregon Health & Science University, Portland, OR, 97239

[2]Genomic Medicine Institute, Lerner Research Institute, Cleveland Clinic, Cleveland, OH 44195

[3]Center for Personalized Genetic Healthcare, Medical Specialties Institute, Cleveland Clinic, Cleveland, OH 44195

[4]Department of Genetics and Genome Sciences, Case Western Reserve University School of Medicine, Cleveland, OH 44106

[‡]Corresponding Authors: fernaale@ohsu.edu; wrighke@ohsu.edu

Summary

Phosphatase and tensin homolog (PTEN) modulates intracellular survival and differentiation signaling pathways downstream of neurotrophin receptors in the developing peripheral nervous system (PNS). Although well-studied in the context of brain development, our understanding of the *in vivo* role of PTEN in the PNS is limited to models of neuropathic pain and nerve injury. Here, we assessed how alterations in PTEN signaling affects the development of peripheral somatosensory circuits. We found that sensory neurons within the dorsal root ganglia (DRG) in *Pten* heterozygous (*Pten*^{Het}) mice exhibit defects in neuronal subtype diversification. Abnormal DRG differentiation in *Pten*^{Het} mice arises early in development, with subsets of neurons

expressing both progenitor and neuronal markers. DRGs in *Pten*^{Het} mice show dysregulation of both mTOR and GSK-3β signaling pathways downstream of PTEN. Finally, we show that mice with an autism-associated mutation in *Pten* (*Pten*$^{Y68H/+}$) show abnormal DRG development. Thus, we have discovered a crucial role for PTEN signaling in the intrinsic diversification of primary sensory neuron populations in the DRG during development.

Running Title

PTEN regulates DRG diversification

Keywords:

PTEN, somatosensory neuron, neuronal differentiation, diversification, DRG, Autism Spectrum Disorder

Introduction

The development of neural circuits depends on tightly regulated signaling pathways that guide the differentiation and diversification of progenitors to establish populations of mature neuronal subtypes [1-7]. Many neurodevelopmental disorders are thought to arise from alterations in neuronal progenitor maintenance and disruptions in the balance between proliferation and differentiation in the central nervous system (CNS) [8]. In contrast, little attention has been given to how altered development of the peripheral nervous system (PNS) contributes to neurodevelopmental disorders.

Neurons in the dorsal root ganglia (DRG) play a critical role in relaying sensory information to the CNS. During embryonic development, neural crest cells (NCCs) delaminate from the dorsal neural tube, migrate laterally, and coalesce to form the nascent DRG. These NCCs are bi-potential progenitors that possess the ability to self-renew and generate both neurons and glia [9]. Through asymmetric divisions, some DRG progenitors exit the cell cycle to initially give rise to transcriptionally diverse populations of sensory neurons, while a subset remains in a proliferative state to subsequently generate satellite glia [10]. There are at least 14 distinct neuronal subtypes in the DRG, each one conveying a specific sensory modality [1, 4, 11, 12]. Neuronal subtype diversity within DRGs is initially established during embryogenesis in overlapping developmental waves of neurogenesis. As postmitotic cells acquire a neuronal fate, they begin to express specific tropomyosin receptor kinase (*Trk*) receptors [13, 14]. In mice, large and medium diameter neurons expressing the neurotrophin receptors TrkC or TrkB are generated first, between embryonic day 9.5 (E9.5) and E11.5, and ultimately differentiate into proprioceptors and

24 mechanoreceptors, respectively [7, 14, 15]. The small diameter neurons that give rise
25 to nociceptors initially express TrkA and are generated between E10.5 and E13.5 [11,
26 15]. Neurotrophin signaling through Trk receptors is required for multiple aspects of
27 DRG neuron development, including neuronal survival, axonal outgrowth, target
28 innervation, and neuronal maturation [13, 16].

29 While the intrinsic molecular pathways downstream of Trk receptors are shared
30 by most DRG neuron populations, how these signals are integrated to regulate fate-
31 specification in sensory neurons *in vivo* is poorly understood [16-18]. The
32 Phosphatidylinositol 3 kinase/protein kinase B/mammalian Target of Rapamycin
33 (PI3K/AKT/mTOR) pathway is one of the main survival and differentiation signaling
34 pathways initiated downstream of Trk receptors in sensory neurons [13, 19-21].
35 Phosphatase and tensin homolog (PTEN) is the primary negative regulator of this
36 pathway, counteracting PI3K activity [22-24]. Dysfunctional or impaired PTEN activity
37 leads to increased AKT and mTOR activation [25]. In humans, germline heterozygous
38 mutations in *PTEN* or other components of the PI3K/AKT/mTOR pathway have been
39 linked to cancer and neurodevelopmental disorders, including autism spectrum
40 disorders (ASD) [26-30]. Moreover, PTEN has been previously shown to have
41 neurodevelopmental roles in mouse models [31]. In the developing CNS, PTEN
42 promotes cell cycle exit and the transition to post-mitotic neuronal fates [32, 33].
43 Heterozygous mutations of *Pten* during development lead to increased cell proliferation
44 and increased production of glial cells [34, 35]. PTEN is also involved in neuronal
45 differentiation [36]. In post-mitotic neurons, PTEN plays a role in axon outgrowth,
46 guidance and branching patterns, and overall neuronal growth [37-40]. When *Pten* is

47 conditionally deleted in neurons, they have hypertrophic cell somas and dendrites in the
48 cerebellum, cortex, and hippocampus [41-43]. At synapses, PTEN regulates dendritic
49 spine density and connectivity [42, 44-46]. Within the PNS, PTEN is involved in growth
50 cone collapse, restricts axon regeneration, and regulates myelin thickness [39, 47, 48].
51 However, despite its well-known function regulating signaling pathways downstream of
52 Trk receptor activation, how alterations in PTEN activity affect neuronal differentiation
53 and population diversity in DRG neurons *in vivo* remains unclear. Moreover, whether
54 heterozygosity of *Pten*, which more accurately models neurodevelopmental disorders, is
55 sufficient to elicit phenotypes in the PNS remains unknown.

56 In this study, we examined DRG development in mice lacking a single copy of
57 wildtype *Pten* ($Pten^{Het}$). We find that adult $Pten^{Het}$ mice have a normal number of DRG
58 neurons, but that population diversification is dramatically altered. These alterations are
59 cell-intrinsic and arise during early stages of neuronal differentiation, with nascent DRG
60 neurons remaining in an intermediate state, expressing both progenitor and neuronal
61 markers simultaneously. We find that both the mTOR and GSK-3β pathways
62 downstream of Akt are dysregulated in $Pten^{Het}$ DRG neurons. Finally, we show that
63 mice harboring a heterozygous ASD-associated mutation that shows predominant
64 nuclear localization ($Pten^{Y68H/+}$) also show alterations in DRG diversification [49-51].
65 Taken together, these results show that tight regulation and proper dosage of PTEN
66 activity is critical for the proper development and diversification of somatosensory
67 neurons *in vivo,* and identify a key contribution of *Pten*-mediated signaling to the
68 development of primary sensory neurons in the context of syndromic ASD.

69

70 **Results**

71 **DRG population diversity is altered in *Pten^{Het}* mice**

72 Recent studies have identified altered development and function of primary DRG
73 neurons in several mouse models of syndromic ASD, including *Mecp2$^{-/y}$*, *Gabrb3$^{+/-}$*,
74 *Shank3$^{+/-}$* and *Fmr1$^{-/y}$* mutants [52-55]. Additionally, single copy mutations in several
75 genes in the PI3K/Akt/mTOR pathway are associated with ASD, and this pathway plays
76 a critical role downstream of Trk receptors [16, 56, 57]. While several studies have
77 focused on the role of PTEN in DRG neurons in the adult or in the context of axon
78 regeneration, how the loss of *Pten* affects DRG development has not been studied *in*
79 *vivo*. To test the hypothesis that disruptions in this pathway affect DRG development,
80 we examined how global loss of a single *Pten* allele (*Pten^{Het}*) affects somatosensory
81 neuron development. We collected hindlimb-innervating DRGs (lumbar level 3-4; L3-L4,
82 **Figure 1A**) from P21 mice and compared the number of neurons in *Pten^{Het}* mutants and
83 wild type (WT; *Pten$^{+/+}$*) littermates using Islet1/2 (ISL1) as a neuronal marker. There was
84 no difference in the total number of ISL1^{+} neurons in the DRG of adult *Pten^{Het}* mutants
85 compared to WT littermate controls (**Figure 1B**). In contrast, when we examined DRGs
86 using subtype-specific markers (**Figure 1C**), we identified alterations in neuronal
87 diversification in *Pten^{Het}* mutants. The number of TrkA^{+} peptidergic nociceptors was
88 decreased by 27% in *Pten^{Het}* mutants relative to control littermates (**Figure 1D**),
89 whereas IB4^{+} non-peptidergic nociceptors were unchanged (**Figure 1E**). In contrast, the
90 Tyrosine Hydroxylase positive (TH+) C-low-threshold mechanoreceptor (C-LTMR)
91 population was increased by 156% (**Figure 1F**). There was no significant change in the

92 number of TrkB$^+$ Aδ-LTMRs or Calbindin$^+$ Aβ-rapidly adapting LTMRs (RA-LTMRs
93 (**Figure 1G, H**). There was also a 56% increase in the number of Parvalbumin positive
94 (PV$^+$) neurons, which includes proprioceptors and populations of low-threshold
95 mechanoreceptors (LTMRs) (**Figure 1I**). Together, these data show that a
96 physiologically optimal expression level of *Pten* is critical for DRG neuron diversification.
97

98 **Control of DRG population diversification by *Pten* is neuron-autonomous**

99 Our examination of *Pten^{Het}* mice identified a role for PTEN in DRG differentiation
100 and population diversification. To test whether this reflected a neuron-autonomous role
101 for PTEN, we asked whether conditional deletion of *Pten* from primary sensory neurons
102 would be sufficient to recapitulate the phenotypes in constitutive *Pten^{Het}* mice. We
103 generated transgenic mice carrying: 1: a *Cre* driver for DRG neurons (*Isl1^{Cre}*); 2: a
104 *Pten^{flox}* allele. We quantified population subtypes in DRGs from *Isl1^{Cre};Pten$^{fl/+}$* animals
105 and *Isl1^{Cre};Pten$^{+/+}$* littermate controls at P21. In line with our results in constitutive
106 *Pten^{Het}* animals, we found that single allele deletion of *Pten* from DRG neurons resulted
107 in altered subtype diversification. There was a 42% decrease in the number of TrkA$^+$
108 peptidergic nociceptors, and no change in the number of IB4$^+$ non-peptidergic
109 nociceptors (**Figure S1A, C, G**). Moreover, we observed a 99% increase in the number
110 of TH$^+$ c-LTMRs in *Pten^{Het}* mutants (**Figure S1B, G**). The number of TrkB+ Aδ-LTMRs
111 and Calbindin+ Aβ RA-LTMR was not affected in mutants, while PV$^+$ neurons were
112 increased by 58% (**Figure S1D, E, F, G**). These data show that PTEN signaling
113 functions within DRG neurons to control their specification and population diversity.
114

115 ***Pten* is essential for regulating neuronal subtype specification during early**
116 **development**

117 To resolve when heterozygous deletion of *Pten* disrupts adult DRG population
118 diversity, we next investigated whether these defects arose early in development or
119 whether they emerged in adult animals. During embryonic development, large/medium
120 diameter neurons expressing TrkC and/or TrkB are generated first, followed by TrkA
121 expressing small diameter neurons [15]. Together, these neurons ultimately give rise to
122 the full complement of genetically and physiologically distinct subtypes of
123 somatosensory neurons (**Figure 2A**). When we examined the proportions of TrkA, TrkB,
124 and TrkC positive neurons between E10.5 and E14.5, we found a significant decrease
125 in the number of $TrkA^+$ neurons in $Pten^{Het}$ mice compared to WT littermates at all ages
126 examined (**Figure 2B**). In contrast, the proportion of $TrkC^+$ neurons was significantly
127 increased between E11.5-E14.5 (**Figure 2D**). In line with our results in adult mice,
128 which did not detect any changes in the proportion of neurons from the TrkB lineage, we
129 saw no change in the number of $TrkB^+$ neurons between E11.5-E14.5 (**Figure 2C**).
130 Therefore, PTEN plays a critical role in the early differentiation of $TrkA^+$ and $TrkC^+$ DRG
131 neurons.

132 To better define the role of PTEN during DRG neuron development, we assessed
133 PTEN's cellular localization by immunostaining DRGs of WT mice between E9.5 and
134 E14.5. At E9.5, when the nascent DRG is primarily comprised of mitotic precursors,
135 PTEN levels are relatively low (**Figure 3A**). PTEN levels sharply increased at E10.5,
136 when DRG neurons are exiting the cell cycle, and remained elevated through E14.5
137 (**Figure 3A**) [58, 59]. We next triple-labeled developing DRGs with PTEN and ISL1 to

138 mark newly differentiated neurons, as well as SOX10 to label DRG precursors and glial
139 cells. At all ages examined, PTEN levels were significantly higher in ISL1^{+} neurons
140 compared to SOX10^{+} cells (**Figure 3B, C**), suggesting that PTEN plays a role in newly
141 generated DRG neurons after they exit the cell cycle.
142
143 **DRG neuron proliferation and apoptosis are normal in the DRG of *Pten^{Het}* mice**
144 The final number of DRG neurons in the adult organism are regulated by a
145 balance of progenitor proliferation and developmental cell death. We therefore used
146 EdU birthdating to examine whether abnormal progenitor proliferation contributed to the
147 altered number of TrkA^{+} and TrkC^{+} neurons observed in *Pten^{Het}* mutants. We
148 administered EdU to pregnant dams at a range of timepoints from E9.5 to E14.5 to mark
149 cells undergoing terminal mitosis at the time of injection. We harvested embryos 2 hours
150 after injection and quantified the proportion of Sox10^{+} progenitors that were EdU
151 positive in DRG sections [60]. There was no difference in the number of EdU^{+}/SOX10^{+}
152 cells at any of the time points examined (**Figure 4A**), suggesting that progenitor
153 proliferation is normal in *Pten^{Het}* mutants.
154 Target-derived neurotrophins binding to Trk receptors activate PI3K/AKT
155 signaling, which regulates pro-survival pathways to ensure the proper number of DRG
156 neurons [6, 61, 62]. Since PTEN functions as a negative regulator of this pathway [63],
157 we expected that we would see increased neuronal survival in mice lacking a single
158 *Pten* allele. Somewhat surprisingly, when we examined activated Caspase-3 in DRGs at
159 a range of timepoints that correspond to the window during which most developmental
160 cell death occurs (E10.5-E14.5), we saw no difference between *Pten^{Het}* mice and WT

161 littermates (**Figure 4B**). Taken together, these data indicate that proliferation and
162 developmental cell death are largely normal in *Pten*^{Het} mice, and are unlikely to
163 significantly contribute to the alterations in DRG subtype diversification.
164
165 ***Pten* heterozygous deletion alters the specification of DRG neurons**
166 Since alterations in DRG subtype populations in *Pten*^{Het} mice do not appear to
167 arise from abnormal proliferation, we carefully examined the transition of neural
168 progenitors to postmitotic neurons. As progenitors in the DRG exit the cell cycle and
169 differentiate into neurons, SOX10 is downregulated and ISL1 levels increase, resulting
170 in largely mutually exclusive expression [9, 64-66]. When we quantified the proportion
171 of SOX10^{+} progenitors and ISL1^{+} neurons in WT and *Pten*^{Het} animals, we observed that
172 proportion of SOX10^{+} progenitors was slightly elevated and the number of ISL1^{+}
173 neurons were slightly reduced in *Pten*^{Het} mice at E12.5 and E13.5, and were not
174 statistically different at any other timepoints (**Figure 5A, B**). However, we observed that
175 while SOX10 and ISL1 are mostly mutually exclusive in WT animals as previously seen
176 [67], there was a significant increase in the proportion of cells co-expressing both
177 progenitor (SOX10) and neuronal (ISL1) markers at every timepoint examined in *Pten*^{Het}
178 animals (**Figure 5A, C**). These results suggest that altering PTEN levels results in
179 abnormal neuronal differentiation in DRG sensory neurons.
180
181 **Intracellular signaling pathways downstream of *Pten* are altered in developing**
182 **sensory neurons in *Pten*^{Het} mutants**

183 We next sought to determine whether specific signaling pathways downstream of
184 PTEN were altered in *Pten* heterozygous mutants. PTEN negatively regulates
185 PI3K/AKT-mediated signaling, which activates both the TSC/mTOR/S6 pathway and the
186 GSK-3β/β-catenin pathway [34, 63, 68] (**Figure 6A**). Since *Pten* haploinsufficiency has
187 different effects on TrkA, TrkB, and TrkC populations within developing DRGs, we
188 examined key readouts downstream of each pathway in developing DRGs by
189 immunostaining for pS6 and using a β-catenin reporter *TCF/Lef:H2B-GFP* mouse
190 crossed onto a $Pten^{Het}$ background (**Figure 6**) [69]. We examined levels of pS6 in
191 cryosections of $Pten^{Het}$ and WT littermates at E11.5, and observed that the number of
192 $pS6^+$/$ISL1^+$ neurons in DRGs of $Pten^{Het}$ embryos was increased (**Figure 6B**). When we
193 co-labeled neurons with antibodies to pS6 and specific Trk receptors, we found that
194 both $TrkA^+$ (**Figure 6C**) and $TrkC^+$ (**Figure 6E**) neurons showed a significant increase in
195 the proportion of $pS6^+$ neurons. Surprisingly, the proportion of $TrkB^+$ neurons that were
196 $pS6^+$ was unchanged in $Pten^{Het}$ embryos (**Figure 6D**).
197 We next used GFP fluorescence in the *TCF/Lef:H2B-GFP* mouse as a readout of
198 activation of the GSK-3β/β-catenin signaling pathway [34, 69]. The number of GFP^+
199 cells that showed activation of β-catenin signaling in E11.5 DRGs was significantly
200 increased in $ISL1^+$ neurons (**Figure 6F**). Examination of population specific markers
201 showed no significant change in the number of $TrkA^+$/GFP^+ and $TrkB^+$/GFP^+ neurons,
202 and a 46% increase in the number of GFP+ neurons within the $TrkC^+$ population
203 (**Figure 6G-I**).
204

205 **DRG neuron diversification is abnormal in mice with an ASD-associated mutation**
206 **in *Pten***.

207 Given the prevalence of *PTEN* mutations within the ASD population and the high
208 incidence of sensory phenotypes in ASD [26, 70], we decided to determine if DRG
209 subtype diversification was impacted by mutations observed in individuals with ASD.
210 The ASD-associated Y68H mutation (*Pten*$^{Y68H/+}$) results in reduced protein stability and
211 nuclear predominant PTEN subcellular localization in CNS neurons [51, 71]. Similar to
212 our results in *Pten*^{Het} mice, *Pten*$^{Y68H/+}$ mice had no change in the total number of DRG
213 neurons, but did have significant alterations in the proportions of specific subtypes
214 (**Figure 7**). Quantification revealed a 50% decrease in the TrkA^{+} peptidergic nociceptive
215 population, a 79% increase in TH^{+} C-LTMRs and a 96% increase in PV^{+} neurons in
216 *Pten*$^{Y68H/+}$ mice when compared to WT littermates (**Figure 7A, C**). There were no
217 changes in the number of IB4^{+} non-peptidergic nociceptors, TrkB^{+} Aδ-LTMRs, or
218 Calbindin^{+} Aβ RA-LTMRs. These numbers are in concordance with our observations in
219 *Pten*^{Het} mice, and suggest that signaling pathways downstream of cytoplasmic PTEN
220 plays a predominant role in regulating DRG subtype diversification.
221

222 **Discussion**

223 *Pten* functions as the primary regulator of PI3K/AKT signaling downstream of
224 neurotrophin receptor activation, however little is known about its role in cell-fate
225 determination and differentiation pathways. Here, we identified a critical developmental
226 role for *Pten* in modulating cell-fate determination in TrkA and TrkC lineages of primary
227 sensory neurons in the DRG.

228

229 **DRG development and the role of *Pten***

230 Primary sensory neurons within DRGs differentiate from neural crest progenitors
231 that delaminate from the dorsal neural tube [7]. Given that there are at least 14
232 molecularly and functionally distinct somatosensory neuron subtypes in adult DRGs, a
233 central question of ongoing investigation is how this neuronal diversity arises during
234 development. Recent work has begun to trace the developmental trajectories and gene
235 expression patterns of each developing population of DRG neurons [3, 4, 72]. As soon
236 as immature DRG neurons exit the cell cycle, they progress through hierarchical steps
237 of specification driven by specific gene expression programs, following specific
238 chronological sequences [1, 3, 4, 73]. The diversity of sensory modalities emerges early
239 in embryonic development through two overlapping waves of sensory neurogenesis that
240 occur between E9.5 and E13 in mice [1, 3, 7, 15, 73]. The first wave (E9.5-E11.5) gives
241 rise to myelinated, medium- and large-diameter neurons which will eventually
242 differentiate into mechanoreceptors, proprioceptors, and a small population of
243 nociceptors [15]. Mechanoreceptors express RET and MAFA and/or TrkB [74],
244 proprioceptors express tropomyosin receptor kinase C (TrkC) and RUNX3 [72], and the
245 small Aδ-nociceptor population expresses TrkA [15, 75, 76]. A second wave of
246 neurogenesis (E10.5-E12.5) generates unmyelinated small-diameter nociceptive
247 neurons [7, 77]. These neurons co-express TrkA and Runx1 and later diversify into
248 pain, itch, thermosensation as well as gentle and, presumably, affective touch [77-79].

249 The identity of each DRG subtype relies on their expression of specific
250 transmembrane receptors and transcription factors [4, 12]. Recent work suggests that

251 counteracting gene-regulatory networks operate within immature postmitotic DRG
252 neurons to establish the transcriptional programs defining neuron subtype-specific fate
253 choice [3]. Extrinsic cues are also necessary for DRG cell-fate determination and
254 transcriptional control of subtype identity [4]. Our understanding of how these intrinsic
255 and extrinsic signaling pathways are integrated and the cellular mechanisms underlying
256 the hierarchical fate-decisions leading to molecular specificity in each DRG neuronal
257 subpopulation remain incomplete. Our data provide evidence that precise regulation of
258 *Pten* signaling plays a critical role in neuronal diversification in DRG neurons. Loss of a
259 single *Pten* allele (*Pten*^{Het}) or incorporation of an ASD-associated mutation in *Pten*
260 (*Pten*$^{Y68H/+}$) leads to significant alterations in the numbers of TrkC- and TrkA-lineage
261 derived populations. These defects are evident as early as E10.5, as developing DRG
262 neurons are acquiring specific fates and persist into adulthood, where the resulting
263 mature neuronal subtypes are affected. Moreover, we show that these defects are
264 modulated intrinsically within the DRG neuron population (*Isl1*^{Cre}*;Pten*$^{Flox/+}$). These
265 results raise a host of new questions, including: 1. *How is Pten signaling contributing to*
266 *cell-fate decisions during development?* 2. *Are neurons in Pten*^{Het} *and Pten*$^{Y68H/+}$ *mice*
267 *only failing to express specific markers, or are these neurons switching fates?* 3. *Does*
268 *altered Pten signaling lead to neurons that are either unspecified or stalled in*
269 *intermediate states?* Further studies using single cell RNA sequencing will help address
270 these questions, and provide additional insight into how reduced *Pten* signaling affects
271 DRG neuron development and function.
272

273 ***Pten* regulates neuronal specification broadly throughout the developing nervous**
274 **system**

275 The current model of neuronal specification in the DRG suggests that nascent
276 neurons are initially unspecified and express a broad array of transcription factors, and
277 progressively acquire molecular specificity through a mechanism of hierarchical binary
278 fate decisions [3, 4]. In other neuronal circuits, *Pten* plays a role in neuronal
279 specification, controlling progenitor cell proliferation to maintain ratios of populations in
280 several lineages [80, 81]. In the retina, *Pten* regulates cell division and is required to
281 produce the full complement of rod photoreceptors and amacrine cells [82]. Moreover,
282 in cortical GABAergic neurons, conditional deletion of *Pten* results in a preferential loss
283 of somatostatin (SST^+) interneurons, leading to an altered ratio of PV^+/SST^+
284 interneurons [36]. Whether this results from changes in transcriptional control of cell-fate
285 determination remains unknown. However, in both retina and developing brain, AKT
286 signaling was found to be increased. Moreover, conditional deletion of the Tuberous
287 Sclerosis Complex (TSC) gene, *Tsc1*, which functions downstream of PTEN and inhibits
288 mTOR, causes ectopic PV expression and altered physiological properties in SST^+
289 cortical interneurons [83]. While these data demonstrate a role for TSC/mTOR signaling
290 events in mediating interneuron differentiation, additional studies have also identified a
291 contribution of the GSK-3β/β-Catenin pathway to cellular organization in the cortex [34].
292 One particularly relevant study showed overactivation of the GSK-3β/β-Catenin and not
293 the mTOR pathway in the developing cortex of *Pten* heterozygous conditional mutants.
294 GSK-3β/β-Catenin overactivation resulted in altered neuronal differentiation and
295 excessive gliogenesis in $Pten^{Het}$ mice [34]. In contrast, homozygous mutants showed

296 overactivation of both the GSK-3β and the mTOR pathway, and lowering mTOR activity
297 was not sufficient to rescue the phenotypes in *Pten*^{Het} mice [34]. More recently, a
298 transcriptomic analysis revealed that, during development, cellular populations within
299 the cerebral cortex have different requirements of PTEN, as heterozygous deletion of
300 *Pten* affects downstream signaling differently in astrocytes and neurons [84]. In our
301 current study, we found that both mTOR and GSK-3β/β-Catenin pathways are
302 hyperactive in TrkC^{+} DRG neurons in *Pten*$^{+/-}$ mutants, whereas only pS6 was
303 significantly elevated in TrkA^{+} DRG neurons. This could reflect differences in
304 downstream signaling in the different populations, or could reflect a lag between β-
305 catenin activity and reporter expression in newly generated TrkA^{+} neurons at E11.5 [80].
306 Along with the different effects of diminished *Pten* signaling in each population
307 subtype derived from the TrkA and TrkC lineages, we saw no changes in population
308 diversification in neurons derived from the TrkB lineage. This particularity of the TrkB
309 lineage may result from a difference in the intrinsic neuronal response to neurotrophins
310 during development. Brain-derived neurotrophin factor (BDNF) signaling through TrkB is
311 qualitatively different than signaling through TrkA and TrkC, and can be regulated by co-
312 factors, modulators, and transactivators including G protein-coupled receptors (GPCRs)
313 and cyclic adenosine monophosphate (cAMP) [85, 86]. Therefore, it is possible that
314 other pathways, along with the PI3K/AKT, are engaged during population diversification
315 within the TrkB lineage, or at least, to modulate the expression of the surface proteins
316 used to identify each population. In this case, either neuronal subtypes derived from the
317 TrkB lineage are unaffected in *Pten*^{Het} mutants, or the phenotypes in these populations
318 are undetectable in our assays.

319

320 ***Pten* regulates gene expression in DRG neurons**

321 A number of studies have examined the consequence of suppressing Pten
322 activity in adult DRGs in the context of axon regeneration following injury [87-91]. While
323 these experiments show that loss of PTEN can promote axon regeneration, the majority
324 of these studies have not examined how this affects the maintenance of DRG neuron
325 identity. However, a recent study showed that inducible deletion of *Pten* from adult
326 DRGs under non-injury conditions results in pathological itch and elevated responses to
327 pruritogens and thermal stimulation [92]. This abnormal sensory response is due in part
328 to ectopic expression of *TRPV1* and *MrgprA3*, particularly within the IB4^{+} population.
329 Simultaneous conditional deletion of *Pten* and *TrpV1* restored itch and thermal
330 responses back to baseline. These results suggest that in addition to the role we have
331 identified for PTEN in regulating DRG subtype differentiation during development,
332 sustained PTEN levels are also required in a subset of adult DRG neurons to maintain
333 their proper molecular identity and function. This prior study only examined the
334 expression of a subset of itch-related genes, so it is not clear what other molecular
335 changes occur in the absence of *Pten* in adult neurons. It is also unknown whether
336 deleting a single allele of *Pten* from adult DRGs is sufficient to alter neuron identity
337 and/or function, as this previous study did not report results from heterozygous *Pten*^{cKO}
338 mice [92].

339 Tuberous Sclerosis Complex 2 (*Tsc2*) functions to negatively modulate mTOR
340 activity downstream of Pten. Conditional deletion of *Tsc2* from developing nociceptors
341 leads to defective innervation of both central and peripheral targets and reduced heat

342 sensitivity and injury-induced cold hypersensitivity [93, 94]. While the overall number of
343 neurons was normal in *Tsc2*^{cKO} mice, there were significant alterations to neuronal
344 subtype populations and gene expression profiles in the DRG. Similar to our results in
345 *Pten*^{Het} and *Pten*$^{Y68H/+}$ mice, they reported a significant decrease in TrkA^{+} neurons in
346 *Tsc2*^{cKO} mice. They also observed an increase in IB4^{+} neurons, which we did not see in
347 our *Pten* mutant mice. This difference may be due to the timing of *Tsc2* deletion
348 (perinatal), or due to the loss of both *Tsc2* alleles, compared to our analysis of *Pten*
349 heterozygous mice. Among the genes that showed altered expression following *Tsc2*
350 deletion, ion channels implicated in DRG neuron function were particularly affected.
351 Whether this reflects abnormal differentiation of neuronal subtypes, or abnormal
352 maintenance of adult subtype identity is unclear.
353

354 **Implications of altered *Pten* signaling during DRG development in autism**
355 **spectrum disorders (ASD)**

356 In addition to the core features of ASD, which include social and communication
357 deficits and repetitive/restrictive interests, it is estimated that up to 90 percent of
358 individuals with ASD experience some form of atypical sensory sensitivity [70]. Recent
359 work has begun to characterize how mutations in ASD-susceptibility genes affect
360 sensory circuit development and/or function [52, 54, 95-100]. Rats with mutations in
361 *Mecp2* show abnormal mechanical and thermal sensitivity due to abnormal sensory
362 neuron development and function during postnatal development [55]. Moreover,
363 deletion of *Mecp2* or *Gabrb3* in somatosensory neurons during development results in
364 tactile deficits, defects in social interactions, and anxiety-like behaviors, all of which are

365 associated with ASD [52]. Pharmacologically reducing tactile overactivity in *Mecp2* and
366 *Shank3* mutants reduced anxiety-like behaviors and some social deficits, further
367 establishing the link between PNS-specific sensory defects and ASD phenotypes [54].
368 Finally, a recent study has emphasized the link between the developmental timing of
369 somatosensory dysfunction and emergence of ASD-like behaviors [53]. Our data
370 showing that primary sensory deficits in $Pten^{Het}$ mutants arise early during development
371 suggest that these defects may contribute to later behavioral abnormalities. Notably, we
372 see the same defects in DRG neuron diversification in both $Pten^{Het}$ and $Pten^{Y68H/+}$ mice.
373 These results show that loss of a single allele of Pten is sufficient to cause defects in
374 DRG diversification, and that this arises predominantly due to the cytosolic signaling
375 function of PTEN. This is supported by the observation that both TSC/mTOR and GSK-
376 3β/β-Catenin signaling pathways are dysregulated in $Pten^{Het}$ DRGs. PTEN also has
377 several functions within the nucleus, and whether these play a role in regulating DRG
378 development remains to be determined. In future studies, the complex cellular functions
379 of PTEN could be genetically dissected using mouse models with mutations affecting
380 distinct functional aspects of PTEN. Furthermore, parsing out how the developmental
381 defects in primary sensory neurons contribute to the wider range of ASD-like
382 phenotypes in $Pten^{Het}$ mutants could be done using conditional deletion of a single copy
383 of *Pten* specifically in DRG neurons.
384

385 Acknowledgements

386 We would like to thank the members of the Wright laboratory for their assistance and
387 discussion throughout the course of this study. Special thanks to Dr. Matthew Pomaville
388 for his insight and help with experimental troubleshooting. We also thank Dr. Martin
389 Riccomagno for his helpful suggestions on the manuscript. This work was supported by
390 NIH grant R01NS091027 (K.M.W.), OHSU Fellowship for Diversity in Research (A.F.),
391 Collins Medical Trust (A.F.) and NIH grant K01NS116168 (A.F.). Confocal microscopy
392 and analysis was performed in the OHSU Advanced Light Microscopy Core, supported
393 by the NIH grant P30NS061800. C.E. is the Sondra J and Stephen R Hardis Chair of
394 Cancer Genomic Medicine at the Cleveland Clinic and would like to thank the Ambrose
395 Monell Foundation.

396

397 **Materials and Methods**

398 **Mouse lines.** All experiments were performed in accordance to OHSU IACUC Protocol
399 #IS00000539. Animals were housed in standard conditions and cared for by the
400 Department of Comparative Medicine at Oregon Health & Science University. Mice
401 were maintained in a 12-hour light/dark cycle, and provided food and water *ad libitum*.
402 For experiments involving embryonic timepoints, noon on the date that a vaginal plug
403 was detected was considered E0.5. For experiments involving constitutive *Pten*
404 heterozygous mice, male $Pten^{Het}$ breeders (*B6;129P2-*$Pten^{tm1Mak}$*/Mmjax* [101]) were
405 crossed with CD1 females to generate experimental mice on a mixed genetic
406 background. For conditional deletion experiments, $Pten^{Flox/+}$ mice ($Pten^{tm1Hwu}$*/J* [102])
407 were crossed to $Isl1^{Cre}$ mice ($Isl1^{tm1(cre)}$*Sev/J* [103]). To examine activation of the GSK-
408 3β/β-Catenin pathway, $Pten^{Het}$ breeders were crossed to a *TCF/Lef:H2B-EGFP* reporter

409 line (*Tg(TCF/Lef1-HIST1H2BB/EGFP)61Hadj/J* [69]). All animals were group housed
410 with littermates and maintained on a mixed genetic background. Mice of both sexes
411 were used for all experiments, and wildtype littermates were used as controls.
412
413 **Proliferation assays.** A single intraperitoneal (IP) injection of EdU in sterile PBS (10μg
414 EdU/g body weight) was given to pregnant dams on one day between E9.5 and E14.5.
415 Two hours after injection, embryos were collected and fixed as described below.
416
417 **Tissue processing and immunolabeling.** All immunolabeling was performed on
418 cryosections following standard protocols [105]. Whole mouse embryos, from litters
419 ranging from E9.5 to E14.5, were fixed overnight at 4°C in 4% paraformaldehyde with
420 gentle agitation. For analysis of P21 DRGs, intact spinal columns were first dissected
421 and fixed overnight at 4°C in 4% paraformaldehyde. The next day, spinal columns were
422 washed in PBS for 30 minutes at room temperature, and spinal cords and attached
423 DRGs were dissected from the spinal column for further processing. All tissue was
424 cryoprotected by incubating in 15% sucrose in PBS for 1 hour, followed by 20% sucrose
425 in PBS overnight at 4°C with gentle agitation. Samples were mounted in OCT and
426 rapidly frozen in methylbutane on dry ice. 20 μm consecutive sections were cut on a
427 Leica CM3050S cryostat, mounted on slides, and allowed to dry for 2 hours at room
428 temperature.
429 For immunolabeling, cryosections mounted on slides were washed 3 times for 5
430 minutes in PBS at room temperature and incubated for 1 hour in blocking solution (5%
431 v/v Normal Donkey Serum, 5% v/v DMSO, 0.25% v/v Triton X-100 in PBS). Slides were

432 then incubated in primary antibodies diluted in blocking solution overnight at 4°C in a
433 humidified staining box. Concentrations for primary antibodies are listed on Table 1.
434 Slides were then washed three times for 5 minutes in PBS, and incubated for 2 hours at
435 room temperature in secondary antibodies diluted at 1:500 in blocking solution. EdU
436 incorporation was detected using Click-iT™ EdU Cell Proliferation Kit for Imaging, Alexa
437 Fluor™ 647 (Cat#C10340). Slides were incubated in EdU detection solution (100 μM
438 Tris pH7.5, 4 mM $CuSO_4$, 5 μM sulfo-Cy5 azide, 100 mM sodium ascorbate) for 30 min
439 at RT, protected from light. Slides were washed 3 times for 10 minutes in PBS, with
440 1:5000 Hoescht added to the second wash to label nuclei. Slides were then
441 coverslipped with Flourmount-G and imaged.
442
443 **Cell counts and statistical analysis.** To quantify immunoreactive DRG neurons, level-
444 matched DRGs from lumbar segments were serially sectioned. For analysis of total
445 number of neurons, sections of entire DRGs were counted. For population proportions,
446 cell proliferation, and cell death assays, 10 consecutive sections of level-matched DRGs
447 were counted. Sections were co-immunostained with antibodies against specific cell
448 makers and Isl1/2. The proportions of each population were calculated by dividing the
449 number of marker-positive cells over the number of total neurons in serial sections from
450 level-matched DRGs of control and mutant mice. Values were averaged for each
451 experiment, with a minimum of 3 animals of mixed sex for each genotype at each
452 timepoint and condition across different litters. The average ± SEM is reported in the
453 figures. Statistical analysis for each experiment was performed by Student's t-test with
454 post-hoc Tukey test. P-values are reported in figure legends and results section.

Table 1: Antibodies used:

Antibody	Species	Supplier	Cat #	RRID	Concentration
Primary Antibodies					
Calbindin	Rabbit	Swant	CB 38	AB_10000340	1:1000
Tyrosine Hydroxylase (TH)	Rabbit	Millipore	AB152	AB_390204	1:1000
TrkA	Goat	Fisher (R&D Systems)	AF1056	AB_2283049	1:100
TrkB	Goat	Fisher (R&D Systems)	AF1494	AB_2155264	1:100
TrkC	Goat	Fisher (R&D Systems)	AF1404	AB_2155412	1:100
Casp3	Rabbit	Cell Signaling	9661S	AB_2341188	1:500
Parvalbumin	Rabbit	Swant	PVG213	AB_2721207	1:1000
Isl1/2	Mouse Igg2b	DHSB	39.4D5	AB_2314683	1:250
GFP	Chicken	Abcam	ab13970	AB_300798	1:1000
Secondary Antibodies					
Anti-Rabbit IgG 488	Donkey	ThermoFisher	A-21206		1:500

Anti-Rabbit IgG 546	Donkey	ThermoFisher	A10040		1:500
Anti-Rabbit IgG 647	Donkey	ThermoFisher	A-31573		1:500
Anti-Mouse Igg2b 488	Goat	ThermoFisher	A-21141		1:500
Anti-Chicken IgY 488	Donkey	Jackson Immuno Research	NC0215979		1:500
Anti-Goat 647	Donkey	ThermoFisher	A-21447		1:500

References:

1. Marmigere, F. and P. Ernfors, *Specification and connectivity of neuronal subtypes in the sensory lineage.* Nat Rev Neurosci, 2007. **8**(2): p. 114-27.
2. Meltzer, S., C. Santiago, N. Sharma, and D.D. Ginty, *The cellular and molecular basis of somatosensory neuron development.* Neuron, 2021. **109**(23): p. 3736-3757.
3. Faure, L., et al., *Single cell RNA sequencing identifies early diversity of sensory neurons forming via bi-potential intermediates.* Nat Commun, 2020. **11**(1): p. 4175.
4. Sharma, N., et al., *The emergence of transcriptional identity in somatosensory neurons.* Nature, 2020. **577**(7790): p. 392-398.
5. Li, C.L., et al., *Somatosensory neuron types identified by high-coverage single-cell RNA-sequencing and functional heterogeneity.* Cell Res, 2016. **26**(1): p. 83-102.
6. Snider, W.D. and I. Silos-Santiago, *Dorsal root ganglion neurons require functional neurotrophin receptors for survival during development.* Philos Trans R Soc Lond B Biol Sci, 1996. **351**(1338): p. 395-403.
7. Ma, Q., C. Fode, F. Guillemot, and D.J. Anderson, *Neurogenin1 and neurogenin2 control two distinct waves of neurogenesis in developing dorsal root ganglia.* Genes Dev, 1999. **13**(13): p. 1717-28.
8. Meechan, D.W., et al., *Modeling a model: Mouse genetics, 22q11.2 Deletion Syndrome, and disorders of cortical circuit development.* Prog Neurobiol, 2015. **130**: p. 1-28.
9. Liu, J.A., et al., *Fbxo9 functions downstream of Sox10 to determine neuron-glial fate choice in the dorsal root ganglia through Neurog2 destabilization.* Proc Natl Acad Sci U S A, 2020. **117**(8): p. 4199-4210.
10. Mapps, A.A., et al., *Diversity of satellite glia in sympathetic and sensory ganglia.* Cell Rep, 2022. **38**(5): p. 110328.
11. Liu, Y. and Q. Ma, *Generation of somatic sensory neuron diversity and implications on sensory coding.* Curr Opin Neurobiol, 2011. **21**(1): p. 52-60.
12. Usoskin, D., et al., *Unbiased classification of sensory neuron types by large-scale single-cell RNA sequencing.* Nat Neurosci, 2015. **18**(1): p. 145-53.
13. Huang, E.J. and L.F. Reichardt, *Trk receptors: roles in neuronal signal transduction.* Annu Rev Biochem, 2003. **72**: p. 609-42.
14. Mu, X., I. Silos-Santiago, S.L. Carroll, and W.D. Snider, *Neurotrophin receptor genes are expressed in distinct patterns in developing dorsal root ganglia.* J Neurosci, 1993. **13**(9): p. 4029-41.
15. Landy, M.A., M. Goyal, and H.C. Lai, *Nociceptor subtypes are born continuously over DRG development.* Dev Biol, 2021. **479**: p. 91-98.
16. Huang, E.J. and L.F. Reichardt, *Neurotrophins: roles in neuronal development and function.* Annu Rev Neurosci, 2001. **24**: p. 677-736.
17. Gorokhova, S., et al., *Uncoupling of molecular maturation from peripheral target innervation in nociceptors expressing a chimeric TrkA/TrkC receptor.* PLoS Genet, 2014. **10**(2): p. e1004081.
18. Segal, R.A. and M.E. Greenberg, *Intracellular signaling pathways activated by neurotrophic factors.* Annu Rev Neurosci, 1996. **19**: p. 463-89.

19. Reichardt, L.F., *Neurotrophin-regulated signalling pathways.* Philos Trans R Soc Lond B Biol Sci, 2006. **361**(1473): p. 1545-64.
20. Postigo, A., et al., *Distinct requirements for TrkB and TrkC signaling in target innervation by sensory neurons.* Genes Dev, 2002. **16**(5): p. 633-45.
21. York, R.D., et al., *Role of phosphoinositide 3-kinase and endocytosis in nerve growth factor-induced extracellular signal-regulated kinase activation via Ras and Rap1.* Mol Cell Biol, 2000. **20**(21): p. 8069-83.
22. Philpott, K.L., M.J. McCarthy, A. Klippel, and L.L. Rubin, *Activated phosphatidylinositol 3-kinase and Akt kinase promote survival of superior cervical neurons.* J Cell Biol, 1997. **139**(3): p. 809-15.
23. Song, W., et al., *ProNGF induces PTEN via p75NTR to suppress Trk-mediated survival signaling in brain neurons.* J Neurosci, 2010. **30**(46): p. 15608-15.
24. Kreis, P., G. Leondaritis, I. Lieberam, and B.J. Eickholt, *Subcellular targeting and dynamic regulation of PTEN: implications for neuronal cells and neurological disorders.* Front Mol Neurosci, 2014. **7**: p. 23.
25. Stambolic, V., et al., *Negative regulation of PKB/Akt-dependent cell survival by the tumor suppressor PTEN.* Cell, 1998. **95**(1): p. 29-39.
26. Tilot, A.K., T.W. Frazier, 2nd, and C. Eng, *Balancing Proliferation and Connectivity in PTEN-associated Autism Spectrum Disorder.* Neurotherapeutics, 2015. **12**(3): p. 609-19.
27. Milella, M., et al., *PTEN: Multiple Functions in Human Malignant Tumors.* Front Oncol, 2015. **5**: p. 24.
28. Buxbaum, J.D., et al., *Mutation screening of the PTEN gene in patients with autism spectrum disorders and macrocephaly.* Am J Med Genet B Neuropsychiatr Genet, 2007. **144B**(4): p. 484-91.
29. Goffin, A., et al., *PTEN mutation in a family with Cowden syndrome and autism.* Am J Med Genet, 2001. **105**(6): p. 521-4.
30. Butler, M.G., et al., *Subset of individuals with autism spectrum disorders and extreme macrocephaly associated with germline PTEN tumour suppressor gene mutations.* J Med Genet, 2005. **42**(4): p. 318-21.
31. Skelton, P.D., R.V. Stan, and B.W. Luikart, *The Role of PTEN in Neurodevelopment.* Mol Neuropsychiatry, 2020. **5**(Suppl 1): p. 60-71.
32. Sun, H., et al., *PTEN modulates cell cycle progression and cell survival by regulating phosphatidylinositol 3,4,5,-trisphosphate and Akt/protein kinase B signaling pathway.* Proc Natl Acad Sci U S A, 1999. **96**(11): p. 6199-204.
33. Lachyankar, M.B., et al., *A role for nuclear PTEN in neuronal differentiation.* J Neurosci, 2000. **20**(4): p. 1404-13.
34. Chen, Y., et al., *Pten Mutations Alter Brain Growth Trajectory and Allocation of Cell Types through Elevated beta-Catenin Signaling.* J Neurosci, 2015. **35**(28): p. 10252-67.
35. Tilot, A.K., et al., *Germline disruption of Pten localization causes enhanced sex-dependent social motivation and increased glial production.* Hum Mol Genet, 2014. **23**(12): p. 3212-27.
36. Vogt, D., et al., *The parvalbumin/somatostatin ratio is increased in Pten mutant mice and by human PTEN ASD alleles.* Cell Rep, 2015. **11**(6): p. 944-956.
37. Huang, W.C., Y. Chen, and D.T. Page, *Hyperconnectivity of prefrontal cortex to amygdala projections in a mouse model of macrocephaly/autism syndrome.* Nat Commun, 2016. **7**: p. 13421.

38. LaSarge, C.L., V.R. Santos, and S.C. Danzer, *PTEN deletion from adult-generated dentate granule cells disrupts granule cell mossy fiber axon structure.* Neurobiol Dis, 2015. **75**: p. 142-50.
39. Chadborn, N.H., et al., *PTEN couples Sema3A signalling to growth cone collapse.* J Cell Sci, 2006. **119**(Pt 5): p. 951-7.
40. Henle, S.J., L.P. Carlstrom, T.R. Cheever, and J.R. Henley, *Differential role of PTEN phosphatase in chemotactic growth cone guidance.* J Biol Chem, 2013. **288**(29): p. 20837-20842.
41. Backman, S.A., et al., *Deletion of Pten in mouse brain causes seizures, ataxia and defects in soma size resembling Lhermitte-Duclos disease.* Nat Genet, 2001. **29**(4): p. 396-403.
42. Kwon, C.H., et al., *Pten regulates neuronal soma size: a mouse model of Lhermitte-Duclos disease.* Nat Genet, 2001. **29**(4): p. 404-11.
43. Kwon, C.H., et al., *Pten regulates neuronal arborization and social interaction in mice.* Neuron, 2006. **50**(3): p. 377-88.
44. Fraser, M.M., I.T. Bayazitov, S.S. Zakharenko, and S.J. Baker, *Phosphatase and tensin homolog, deleted on chromosome 10 deficiency in brain causes defects in synaptic structure, transmission and plasticity, and myelination abnormalities.* Neuroscience, 2008. **151**(2): p. 476-88.
45. Williams, M.R., et al., *Hyperactivity of newborn Pten knock-out neurons results from increased excitatory synaptic drive.* J Neurosci, 2015. **35**(3): p. 943-59.
46. Xiong, Q., H.V. Oviedo, L.C. Trotman, and A.M. Zador, *PTEN regulation of local and long-range connections in mouse auditory cortex.* J Neurosci, 2012. **32**(5): p. 1643-52.
47. Christie, K.J., et al., *PTEN inhibition to facilitate intrinsic regenerative outgrowth of adult peripheral axons.* J Neurosci, 2010. **30**(27): p. 9306-15.
48. Cotter, L., et al., *Dlg1-PTEN interaction regulates myelin thickness to prevent damaging peripheral nerve overmyelination.* Science, 2010. **328**(5984): p. 1415-8.
49. Lobo, G.P., et al., *Germline and somatic cancer-associated mutations in the ATP-binding motifs of PTEN influence its subcellular localization and tumor suppressive function.* Hum Mol Genet, 2009. **18**(15): p. 2851-62.
50. He, X., et al., *Naturally occurring germline and tumor-associated mutations within the ATP-binding motifs of PTEN lead to oxidative damage of DNA associated with decreased nuclear p53.* Hum Mol Genet, 2011. **20**(1): p. 80-9.
51. Sarn, N., S. Thacker, H. Lee, and C. Eng, *Germline nuclear-predominant Pten murine model exhibits impaired social and perseverative behavior, microglial activation, and increased oxytocinergic activity.* Mol Autism, 2021. **12**(1): p. 41.
52. Orefice, L.L., et al., *Peripheral Mechanosensory Neuron Dysfunction Underlies Tactile and Behavioral Deficits in Mouse Models of ASDs.* Cell, 2016. **166**(2): p. 299-313.
53. Tasnim, A., et al., *The developmental timing of spinal touch processing alterations and its relation to ASD-associated behaviors in mouse models.* bioRxiv, 2023: p. 2023.05.09.539589.
54. Orefice, L.L., et al., *Targeting Peripheral Somatosensory Neurons to Improve Tactile-Related Phenotypes in ASD Models.* Cell, 2019. **178**(4): p. 867-886 e24.
55. Bhattacherjee, A., et al., *Neuronal cytoskeletal gene dysregulation and mechanical hypersensitivity in a rat model of Rett syndrome.* Proc Natl Acad Sci U S A, 2017. **114**(33): p. E6952-E6961.

56. Segal, R.A., *Selectivity in neurotrophin signaling: theme and variations.* Annu Rev Neurosci, 2003. **26**: p. 299-330.
57. Thomas, S.D., N.K. Jha, S. Ojha, and B. Sadek, *mTOR Signaling Disruption and Its Association with the Development of Autism Spectrum Disorder.* Molecules, 2023. **28**(4).
58. Lawson, S.N. and T.J. Biscoe, *Development of mouse dorsal root ganglia: an autoradiographic and quantitative study.* J Neurocytol, 1979. **8**(3): p. 265-74.
59. Venteo, S., et al., *Neurog2 Deficiency Uncovers a Critical Period of Cell Fate Plasticity and Vulnerability among Neural-Crest-Derived Somatosensory Progenitors.* Cell Rep, 2019. **29**(10): p. 2953-2960 e2.
60. Serinagaoglu, Y., J. Pare, M. Giovannini, and X. Cao, *Nf2-Yap signaling controls the expansion of DRG progenitors and glia during DRG development.* Dev Biol, 2015. **398**(1): p. 97-109.
61. Klesse, L.J. and L.F. Parada, *p21 ras and phosphatidylinositol-3 kinase are required for survival of wild-type and NF1 mutant sensory neurons.* J Neurosci, 1998. **18**(24): p. 10420-8.
62. Datta, S.R., et al., *Akt phosphorylation of BAD couples survival signals to the cell-intrinsic death machinery.* Cell, 1997. **91**(2): p. 231-41.
63. Georgescu, M.M., *PTEN Tumor Suppressor Network in PI3K-Akt Pathway Control.* Genes Cancer, 2010. **1**(12): p. 1170-7.
64. Zhang, Q., et al., *Temporal requirements for ISL1 in sympathetic neuron proliferation, differentiation, and diversification.* Cell Death Dis, 2018. **9**(2): p. 247.
65. McKeown, S.J., et al., *Sox10 overexpression induces neural crest-like cells from all dorsoventral levels of the neural tube but inhibits differentiation.* Dev Dyn, 2005. **233**(2): p. 430-44.
66. Sonnenberg-Riethmacher, E., et al., *Development and degeneration of dorsal root ganglia in the absence of the HMG-domain transcription factor Sox10.* Mech Dev, 2001. **109**(2): p. 253-65.
67. Sun, Y., et al., *A central role for Islet1 in sensory neuron development linking sensory and spinal gene regulatory programs.* Nat Neurosci, 2008. **11**(11): p. 1283-93.
68. Huang, W., et al., *GSK3 beta mediates suppression of cyclin D2 expression by tumor suppressor PTEN.* Oncogene, 2007. **26**(17): p. 2471-82.
69. Ferrer-Vaquer, A., et al., *A sensitive and bright single-cell resolution live imaging reporter of Wnt/ss-catenin signaling in the mouse.* BMC Dev Biol, 2010. **10**: p. 121.
70. Ben-Sasson, A., et al., *A meta-analysis of sensory modulation symptoms in individuals with autism spectrum disorders.* J Autism Dev Disord, 2009. **39**(1): p. 1-11.
71. Han, S.Y., et al., *Functional evaluation of PTEN missense mutations using in vitro phosphoinositide phosphatase assay.* Cancer Res, 2000. **60**(12): p. 3147-51.
72. Dietrich, S., et al., *Molecular identity of proprioceptor subtypes innervating different muscle groups in mice.* Nat Commun, 2022. **13**(1): p. 6867.
73. Lallemend, F. and P. Ernfors, *Molecular interactions underlying the specification of sensory neurons.* Trends Neurosci, 2012. **35**(6): p. 373-81.
74. Bourane, S., et al., *Low-threshold mechanoreceptor subtypes selectively express MafA and are specified by Ret signaling.* Neuron, 2009. **64**(6): p. 857-70.
75. Lawson, S.N., X. Fang, and L. Djouhri, *Nociceptor subtypes and their incidence in rat lumbar dorsal root ganglia (DRGs): focussing on C-polymodal nociceptors, Abeta-*

nociceptors, moderate pressure receptors and their receptive field depths. Curr Opin Physiol, 2019. **11**: p. 125-146.
76. Fang, X., et al., *trkA is expressed in nociceptive neurons and influences electrophysiological properties via Nav1.8 expression in rapidly conducting nociceptors.* J Neurosci, 2005. **25**(19): p. 4868-78.
77. Marmigere, F., et al., *The Runx1/AML1 transcription factor selectively regulates development and survival of TrkA nociceptive sensory neurons.* Nat Neurosci, 2006. **9**(2): p. 180-7.
78. Luo, W., et al., *A hierarchical NGF signaling cascade controls Ret-dependent and Ret-independent events during development of nonpeptidergic DRG neurons.* Neuron, 2007. **54**(5): p. 739-54.
79. Keeler, A.B., et al., *A developmental atlas of somatosensory diversification and maturation in the dorsal root ganglia by single-cell mass cytometry.* Nat Neurosci, 2022. **25**(11): p. 1543-1558.
80. Sun, C., et al., *PTEN regulation of the proliferation and differentiation of auditory progenitors through the PTEN/PI3K/Akt-signaling pathway in mice.* Neuroreport, 2014. **25**(3): p. 177-83.
81. Lyu, J., et al., *The protein phosphatase activity of PTEN is essential for regulating neural stem cell differentiation.* Mol Brain, 2015. **8**: p. 26.
82. Tachibana, N., et al., *Pten Regulates Retinal Amacrine Cell Number by Modulating Akt, Tgfbeta, and Erk Signaling.* J Neurosci, 2016. **36**(36): p. 9454-71.
83. Malik, R., et al., *Tsc1 represses parvalbumin expression and fast-spiking properties in somatostatin lineage cortical interneurons.* Nat Commun, 2019. **10**(1): p. 4994.
84. Cheung, S.K.K., et al., *Neuropathological signatures revealed by transcriptomic and proteomic analysis in Pten-deficient mouse models.* Sci Rep, 2023. **13**(1): p. 6763.
85. Andreska, T., P. Luningschror, and M. Sendtner, *Regulation of TrkB cell surface expression-a mechanism for modulation of neuronal responsiveness to brain-derived neurotrophic factor.* Cell Tissue Res, 2020. **382**(1): p. 5-14.
86. Mitre, M., et al., *Transactivation of TrkB Receptors by Oxytocin and Its G Protein-Coupled Receptor.* Front Mol Neurosci, 2022. **15**: p. 891537.
87. Danilov, C.A. and O. Steward, *Conditional genetic deletion of PTEN after a spinal cord injury enhances regenerative growth of CST axons and motor function recovery in mice.* Exp Neurol, 2015. **266**: p. 147-60.
88. Willenberg, R., et al., *Variable laterality of corticospinal tract axons that regenerate after spinal cord injury as a result of PTEN deletion or knock-down.* J Comp Neurol, 2016. **524**(13): p. 2654-76.
89. Park, K.K., et al., *Promoting axon regeneration in the adult CNS by modulation of the PTEN/mTOR pathway.* Science, 2008. **322**(5903): p. 963-6.
90. Liu, K., et al., *PTEN deletion enhances the regenerative ability of adult corticospinal neurons.* Nat Neurosci, 2010. **13**(9): p. 1075-81.
91. Chandran, V., et al., *A Systems-Level Analysis of the Peripheral Nerve Intrinsic Axonal Growth Program.* Neuron, 2016. **89**(5): p. 956-70.
92. Hu, L., et al., *The role of PTEN in primary sensory neurons in processing itch and thermal information in mice.* Cell Rep, 2022. **39**(3): p. 110724.
93. Carlin, D., et al., *Deletion of Tsc2 in Nociceptors Reduces Target Innervation, Ion Channel Expression, and Sensitivity to Heat.* eNeuro, 2018. **5**(2).

94. Abe, N., et al., *Mammalian target of rapamycin (mTOR) activation increases axonal growth capacity of injured peripheral nerves.* J Biol Chem, 2010. **285**(36): p. 28034-43.
95. Price, T.J. and O.K. Melemedjian, *Fragile X mental retardation protein (FMRP) and the spinal sensory system.* Results Probl Cell Differ, 2012. **54**: p. 41-59.
96. He, C.X., et al., *Tactile Defensiveness and Impaired Adaptation of Neuronal Activity in the Fmr1 Knock-Out Mouse Model of Autism.* J Neurosci, 2017. **37**(27): p. 6475-6487.
97. Chelini, G., et al., *Aberrant Somatosensory Processing and Connectivity in Mice Lacking Engrailed-2.* J Neurosci, 2019. **39**(8): p. 1525-1538.
98. Deng, P.Y., O. Avraham, V. Cavalli, and V.A. Klyachko, *Hyperexcitability of Sensory Neurons in Fragile X Mouse Model.* Front Mol Neurosci, 2021. **14**: p. 796053.
99. Han, Q., et al., *SHANK3 Deficiency Impairs Heat Hyperalgesia and TRPV1 Signaling in Primary Sensory Neurons.* Neuron, 2016. **92**(6): p. 1279-1293.
100. Dawes, J.M., et al., *Immune or Genetic-Mediated Disruption of CASPR2 Causes Pain Hypersensitivity Due to Enhanced Primary Afferent Excitability.* Neuron, 2018. **97**(4): p. 806-822 e10.
101. Suzuki, A., et al., *High cancer susceptibility and embryonic lethality associated with mutation of the PTEN tumor suppressor gene in mice.* Curr Biol, 1998. **8**(21): p. 1169-78.
102. Lesche, R., et al., *Cre/loxP-mediated inactivation of the murine Pten tumor suppressor gene.* Genesis, 2002. **32**(2): p. 148-9.
103. Yang, L., et al., *Isl1Cre reveals a common Bmp pathway in heart and limb development.* Development, 2006. **133**(8): p. 1575-85.
104. Madisen, L., et al., *A robust and high-throughput Cre reporting and characterization system for the whole mouse brain.* Nat Neurosci, 2010. **13**(1): p. 133-40.
105. Pomaville, M.B. and K.M. Wright, *Follicle-innervating Adelta-low threshold mechanoreceptive neurons form receptive fields through homotypic competition.* Neural Dev, 2023. **18**(1): p. 2.

Figure 1. Population diversity in DRGs is altered in *Pten^{Het}* mice. A) Schematic representation of spinal cord with attached DRGs. All quantifications were done in L4 DRGs in P21 animals. **B)** Images and quantification of total number of neurons using ISL1 as a marker. Total number of neurons was the same in WT and *Pten^{Het}* mutants (n=3, p=0.57, Student's t-test). **C)** Schematic of DRG primary sensory neuron diversity subpopulations of proprioceptors, mechanoreceptors and nociceptors are labeled with each of the markers outlined in schematic. **D-I)** Representative images of cryosections of WT and *Pten^{Het}* adult DRGs with specific markers (left panels) and quantification (right panels). Inserts show magnification of squared area. **D)** TrkA positive peptidergic nociceptors are decreased in *Pten^{Het}* mutants (n=3, p<0.002, Student's t-test). **E)** Quantification of IB4-positive non-peptidergic nociceptors (right panel) shows no change in *Pten^{Het}* mutants compared to WT controls (n=3, p=0.20, Student's t-test). **F)** Tyrosine hydroxylase (TH) positive LTMRs are increased in *Pten^{Het}* mutants compared to WT littermates (n=3, p<0.05, Student's t-test). **G-H)** There were no significant changes in the number of TrkB-lineage mechanoreceptors (TrkB+ Aδ-LTMRs:, n=3, p=0.34, Student's t-test; Calbindin+ Aβ RA-LTMR: n=3, p=0.41, Student's t-test). **I)** Parvalbumin positive (PV+) proprioceptors were increased in *Pten^{Het}* mutants compared to WT littermates (n=3 p<0.002, Student's t-test).

Figure S1: Control of population diversification by *Pten* is neuron-autonomous.

A-F) Representative images of cryosections of DRGs from P21 *Isl1*^{Cre}*;Pten*$^{fl/+}$ and control littermates with specific markers. **G)** Quantification of proportions of each population subtypes in *Isl1*^{Cre}*;Pten*$^{fl/+}$ normalized to control. TrkA+ peptidergic nociceptors are reduced in *Isl1*^{Cre}*;Pten*$^{fl/+}$ mutants (n=3 $p<0.015$, Student's t-test). IB4+ non-peptidergic nociceptors were unchanged in mutants when compared to controls (n=3, $p=0.69$, Student's t-test).TH+ c-LTMRs show an increase in *Isl1*^{Cre}*;Pten*$^{fl/+}$ mutants compared to controls (n=3, $p<0.001$, Student's t-test). There were no significant changes in the number of TrkB+ or Calb1+ mechanoreceptors (TrkB: n=3, $p=0.83$; Calb1: n=3, $p=0.49$, Student's t-test). PV+ neurons showed an increase in *Isl1*^{Cre}*;Pten*$^{fl/+}$ mutants compared to controls (n=3 $p<0.05$, Student's t-test).

Figure 2: Neuronal population diversity is altered in *Pten^{Het}* mutants throughout development. A) Schematic of DRG primary sensory neuron diversification during development. Neural crest cells (NCCs) differentiate and diversify into subpopulations that give rise to proprioceptors, mechanoreceptors, and nociceptors; schematic shows markers for specific subpopulations. **B-D)** Representative images of cryosections of WT and *Pten^{Het}* E11.5 DRGs with markers of each subtype (left panels) and quantification (right panels). **B)** Representative images of DRGs labeled with TrkA (left), quantification (right) shows a decrease in the number of TrkA positive neurons in *Pten^{Het}* mutants throughout development (n=3, E10.5: $p<0.004$; E11.5 : $p<0.03$; E12.5: $p<0.02$, E13.5: $p<0.045$, E14.5: $p<0.03$, Student's t-test). **C)** Images showing DRGs labeled with TrkB (left), quantification (right) shows no changes the number of TrkB+ neurons in *Pten^{Het}* mutants (n=3, E10.5: $p=0.46$; E11.5: $p=0.32$; E12.5: $p=0.45$; E13.5: $p=0.47$; E14.5: $p=0.28$, Student's t-test). **D)** Images of E11.5 DRGs labeled with TrkC (left), quantification (right) shows an increase in the proportion of TrkC+ neurons in *Pten^{Het}* mutants after E10.5 (E10.5: $p=0.14$; E11.5 $p<0.02$; E12.5: $p<0.05$; E13.5: $p<0.05$; E14.5: $p<0.01$, Student's t-test).

Figure 3: Pten levels are elevated in newly generated DRG neurons. A) Representative images of embryonic DRGs (left to right from E9.5-14.5) of WT animals labeled with PTEN by immunohistochemistry. At E9.5, when nascent DRGs are primarily compromised of mitotic precursors, PTEN levels are relatively low. PTEN levels rise sharply at E10.5 and E11.5, as the majority of DRG neurons differentiate. **B)** Representative images of embryonic DRGs (left to right, from E10.5 to E14.5) labeled by immunofluorescence with antibodies against PTEN, Islet1/2 (Isl1/2) and Sox10. Arrows indicate Sox10+ progenitors, which are not Isl1/2+ or Pten+. **C)** Quantification of the average intensity levels of PTEN within Isl1/2+ neurons and Sox10+ positive precursors. At all ages, PTEN levels were significantly higher in Isl1/2+ neurons compared to Sox10+ progenitors (n=3, E10.5: $p<0.03$; E11.5: $p<0.001$; E12.5: $p<0.02$; E13.5: $p<0.01$; E14.5: $p<0.02$; Student's t-test).

Figure 4: Proliferation and developmental cell death are normal in *Pten^{Het}* mutants. A) Representative images of E11.5 DRGs from WT and *Pten^{Het}* littermates birth-dated with EdU and labeled with Sox10 immunostaining (left panels). Quantification (right panel) shows percentage of Sox10+ progenitors undergoing proliferation at each developmental time point (E9.5-E14.5). At all ages quantified, there is no difference in the percentage of EdU+;Sox10+ precursors in *Pten^{Het}* compared to WT controls (n=3, E9.5: p=0.055; E10.5: p=0.11; E11.5: p=0.45; E12.5: p=0.06; E13.5: p=0.484; E14.5: p=0.481, at E14.5; Student's t-test). **B)** Representative images from E11.5 DRGs of WT and *Pten^{Het}* littermates showing activated Caspase 3 (Casp3; green) and Islet 1/2 immunoreactivity (left panels). Quantification (right panel) shows percentage of Isl1/2+ neurons co-labeled with activated Caspase 3. At all ages quantified (E10.5- E14.5), there is no difference in the percentage of activated Casp3+;Islet1+ neurons in *Pten^{Het}* DRGs compared to WT controls (n=3, E10.5: p=0.54; E11.5: p=0.16; at E12.5: p=0.069; at E13.5: p=0.91; at E14.5: p=0.84, Student's t-test).

Figure 5: Progression of neuronal progenitors to neurons is altered in *Pten^{Het}* mutants. A) Representative images of E12.5 DRGs from WT and *Pten^{Het}* littermates co-stained with markers of neuronal progenitors (Sox10) and neurons (Isl1/2). **B)** Quantification of proportions of neuronal precursors (left) and neurons (right) within DRGs of WT and *Pten^{Het}* littermates at different developmental ages from E9.5 to E14.5. At E12.5 and E13.5 there was a small significant increase in the proportion of Sox10+ progenitors and a corresponding decrease in the proportion of Isl1/2+ neurons in *Pten^{Het}* mutants (n=3, E9.5: $p=0.13$; E10.5: $p=0.48$; E11.5: $p=0.45$; E12.5: $p<0.04$; E13.5: $p<0.03$; E14.5: $p=0.28$, Student's t-test). **C)** Quantification of the proportion of cells co-labeled with markers for neuronal precursors (Sox10) and neurons (Isl1/2) from E9.5 to E14.5. The proportion of cells that were both Sox10+ and Isl1/2+ increased dramatically in *Pten^{Het}* mice compared to WT littermates at each timepoint examined (n=3, E9.5: $p<0.02$; E10.5: $p<0.04$; E11.5: $p<0.001$; E12.5: $p<0.001$; E13.5: $p<0.001$; E14.5: $p<0.04$, Student's t-test).

Figure 6: Altered signaling downstream of PI3K/AKT in TrkA and TrkC lineages in *Pten^{Het}* mutants. A) Schematic representation of mTOR and GSK-3β signaling pathways downstream of PI3K/AKT. **B-E)** Representative images (left) and quantification (right) of E11.5 DRGs of WT and *Pten^{Het}* littermates immunolabeled with Isl1 (B) TrkA (C) TrkB (D) or TrkC (E) and phospho-S6 (pS6) to measure activity of the PI3K/AKT/mTOR pathway. **B)** Quantification (right) shows an increase in the proportion of pS6+/Isl1+ neurons in *Pten^{Het}* compared to WT (n=3, p<0.041, Student's t-test). **C)** Within the TrkA population, pS6+/TrkA+ neurons were increased in *Pten^{Het}* compared to WT littermates (n=3, p<0.02, Student's t-test). **D)** Quantification in TrkB+ neurons (right) shows no significant change in the proportions of pS6+/TrkB+ neurons between *Pten^{Het}* and WT controls (n=3, p=0.82, Student's t-test). **E)** Quantification shows increased number of pS6+/TrkC+ neurons in *Pten^{Het}* compared to WT littermates (n=3, p<0.03, Student's t-test). **F-I)** Representative images (left) and quantification (right) of E11.5 DRGs from *TCF/Lef:H2B-GFP*;*Pten^{Het}* DRGs and control littermates immunolabeled with Isl1 (F) TrkA (H) TrkB (H) or TrkC (I) to measure activity of the GSK-3β/β-catenin pathway. **F)** The proportion of GFP+/Isl1+ neurons was increased in *TCF/Lef:H2B-GFP;Pten^{Het}* when compared to controls (n=3, p<0.005, Student's t-test). **G)** Within the TrkA population, there was no significant change in the number of GFP+/TrkA+ neurons between *TCF/Lef:H2B-GFP*;*Pten^{Het}* and *TCF/Lef:H2B-GFP*;*Pten^{WT}* controls (n=3, p=0.11, Student's t-test). **H)** There was no significant change in the proportion of GFP+/TrkB+ neurons between *TCF/Lef:H2B-GFP*;*Pten^{Het}* and *TCF/Lef:H2B-GFP*;*Pten^{WT}* WT controls (p=0.96, Student's t-test). **I)** The TrkC lineage shows a 127%

increase in GFP+/TrkC+ neurons in *TCF/Lef:H2B-GFP*;*Pten*^{Het} compared to *TCF/Lef:H2B-GFP*;*Pten*^{WT} controls (n=3, $p<0.002$, Student's t-test).

Figure 7: DRG neuron diversification is abnormal in *Pten*$^{Y68H/+}$ mice. A) Representative images of cryosections of WT (top row) and *Pten*^{Y68H} (bottom row) P21 DRGs labeled with specific markers for select DRG subtypes. Inserts show magnification of squared area. **B)** The total number of Isl1/2+ DRG neurons was not altered in *Pten*^{Y68H} mutants compared to WT controls (n=3 p=0.18, Student's t-test). **C)** Quantification shows that the number of TrkA+ peptidergic nociceptors is decreased in *Pten*^{Y68H} mutants (n=3 p<0.04, Student's t-test), whereas TH+ c-LTMRs and PV+ neurons are increased in *Pten*^{Y68H} mutants (TH: n=3 p<0.005, PV: n=3 p<0.02, Student's t-test). There was no significant difference in the number of IB4+ non-peptidergic nociceptors, TrkB+ Aδ-LTMRs, or Calb1+ Aβ-LTMRs in *Pten*^{Y68H} mutants compared to WT littermates (IB4: n=3 p=0.09, TrkB: n=3 p=0.47; Calb1: n=3 p=0.38, Student's t-test).

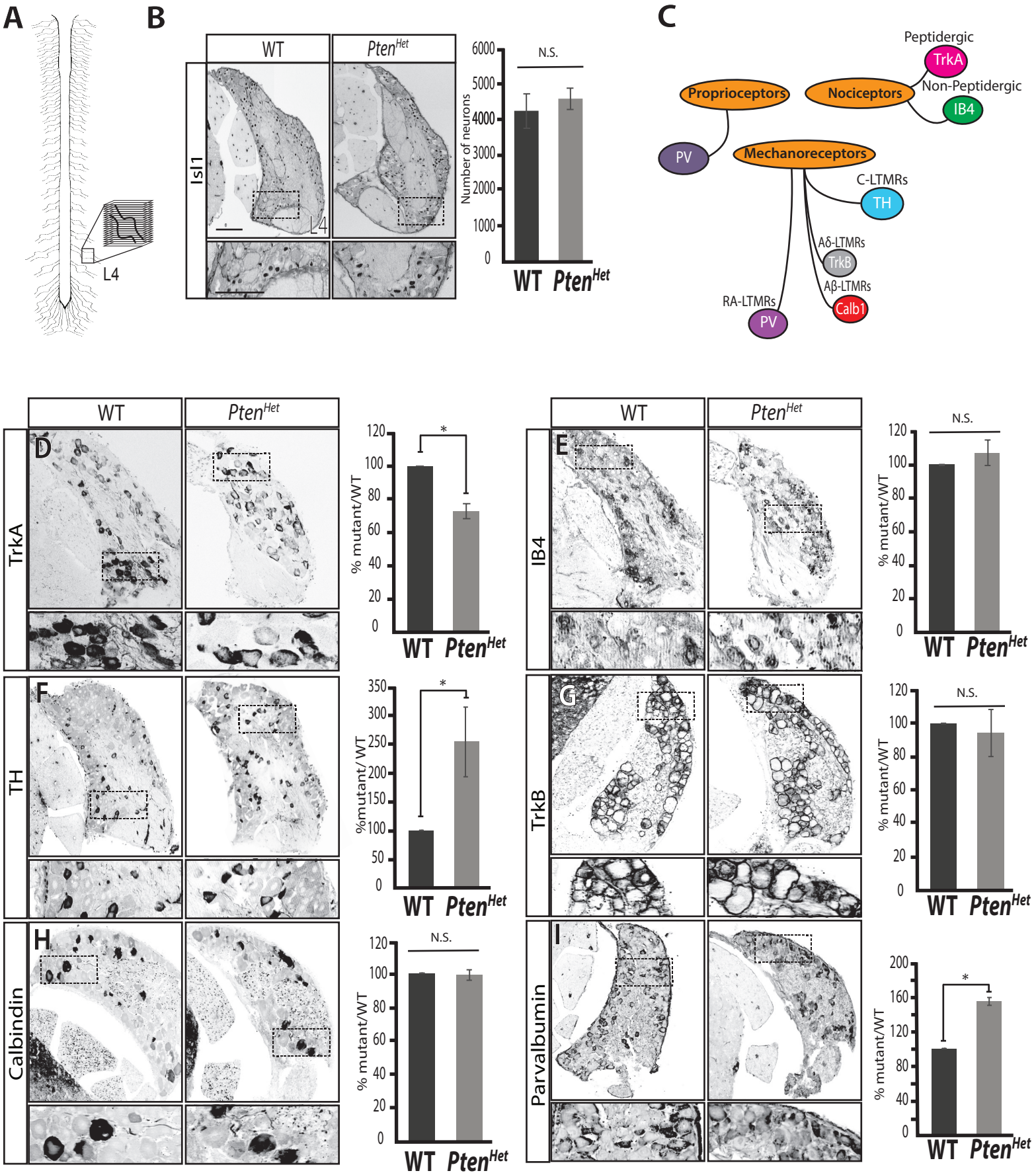
A
L4
B
WT
Pten^Het
Isl1
L4
Number of neurons
N.S.
WT
Pten^Het
C
Peptidergic
TrkA
Non-Peptidergic
IB4
Proprioceptors
Nociceptors
PV
Mechanoreceptors
C-LTMRs
TH
Aδ-LTMRs
TrkB
Aβ-LTMRs
Calb1
RA-LTMRs
PV
D
TrkA
% mutant/WT
*
E
IB4
N.S.
F
TH
%mutant/ WT
*
G
TrkB
N.S.
H
Calbindin
N.S.
I
Parvalbumin
*

Figure 1

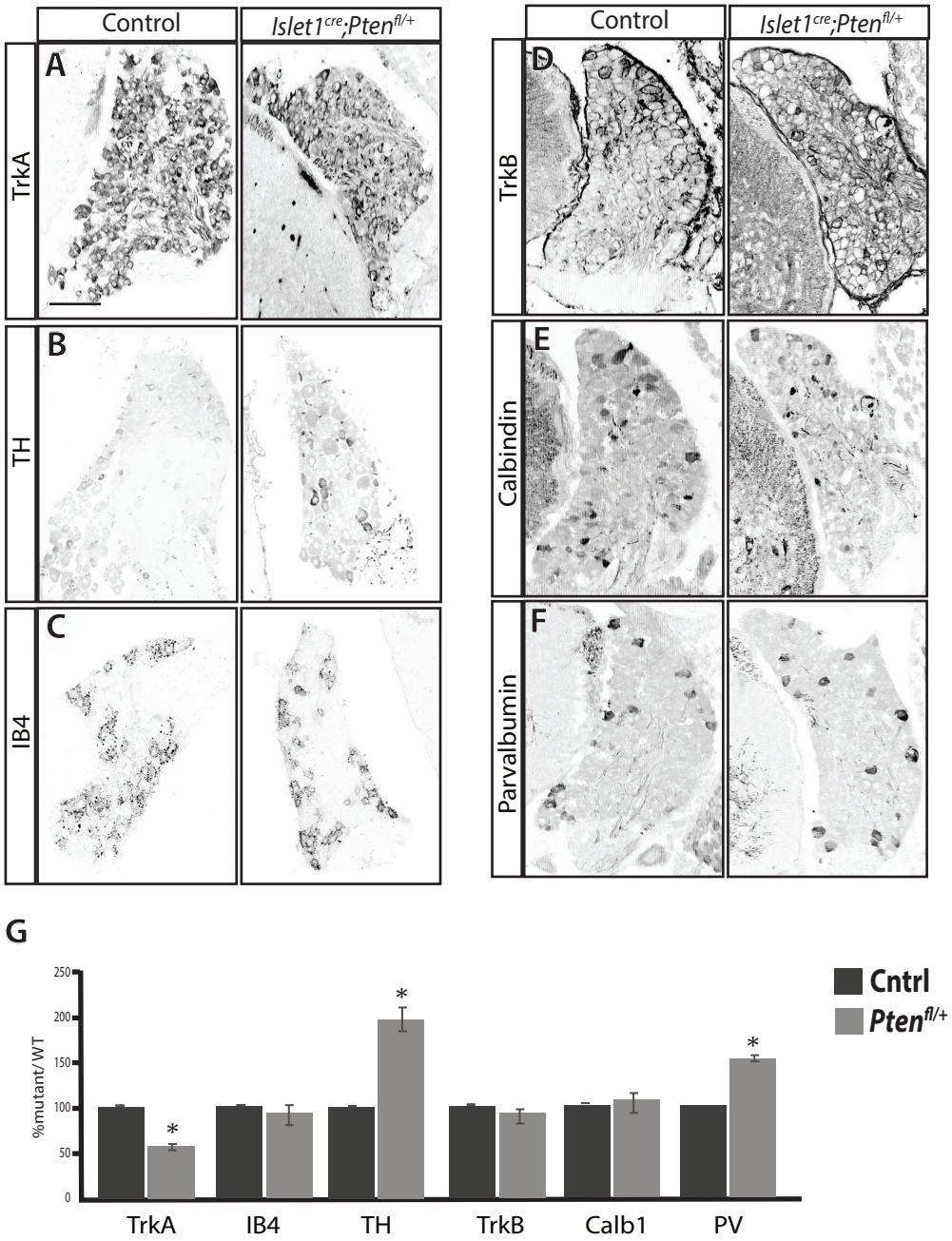
Control
Islet1cre;Ptenfl/+
A
TrkA
B
TH
C
IB4
Control
Islet1cre;Ptenfl/+
D
TrkB
E
Calbindin
F
Parvalbumin
G
Cntrl
Ptenfl/+
%mutant/WT
250
200
150
100
50
0
*
*
*
TrkA
IB4
TH
TrkB
Calb1
PV

Figure S1

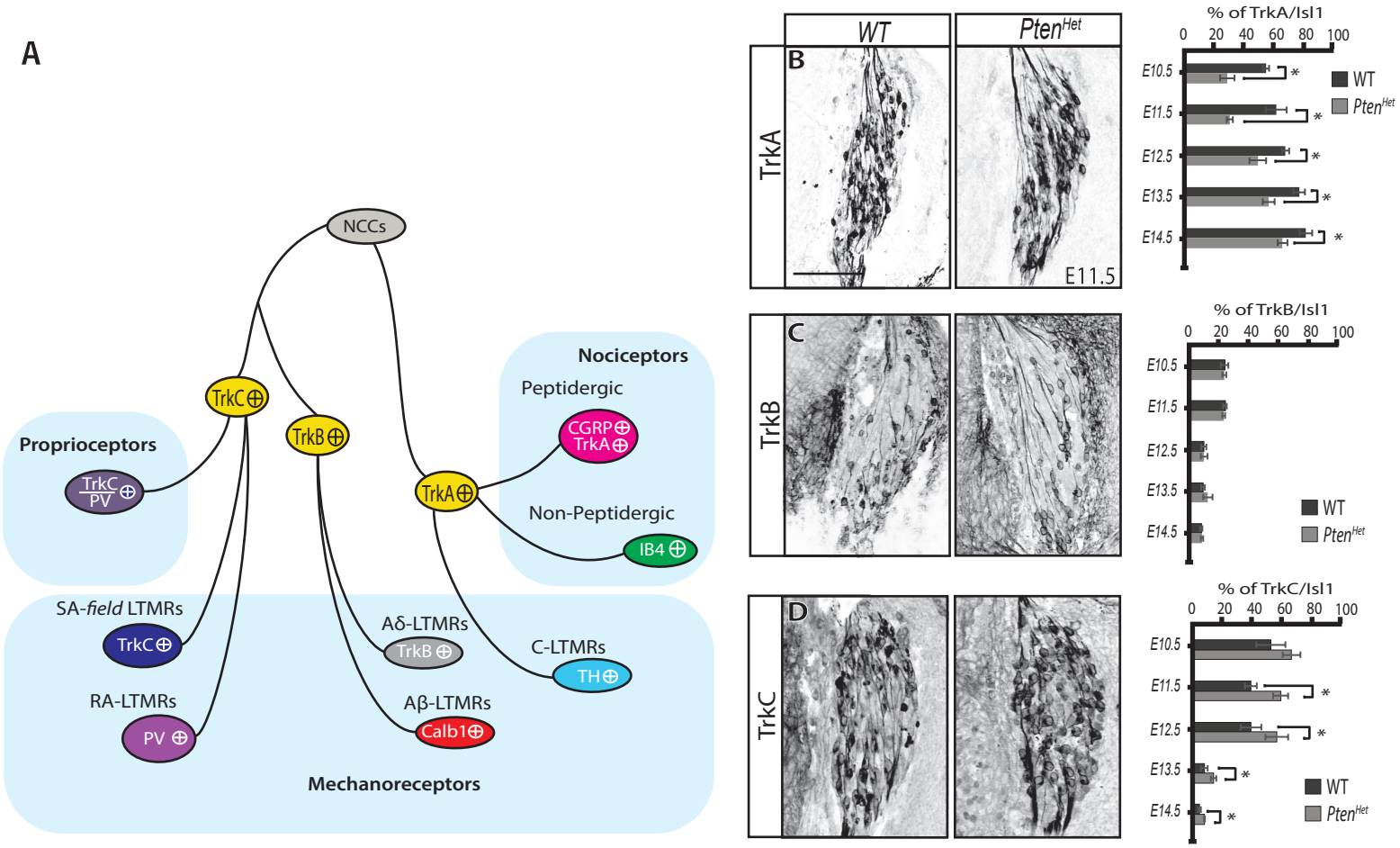
A
NCCs
TrkC⊕
TrkB⊕
TrkA⊕
Proprioceptors
TrkC PV ⊕
Nociceptors
Peptidergic
CGRP⊕ TrkA⊕
Non-Peptidergic
IB4 ⊕
SA-field LTMRs
TrkC ⊕
RA-LTMRs
PV ⊕
Aδ-LTMRs
TrkB ⊕
Aβ-LTMRs
Calb1⊕
C-LTMRs
TH⊕
Mechanoreceptors
WT
Pten Het
B
TrkA
E11.5
C
TrkB
D
TrkC
% of TrkA/Isl1
% of TrkB/Isl1
% of TrkC/Isl1
0 20 40 60 80 100
E10.5
E11.5
E12.5
E13.5
E14.5
WT
Pten Het

Figure 2

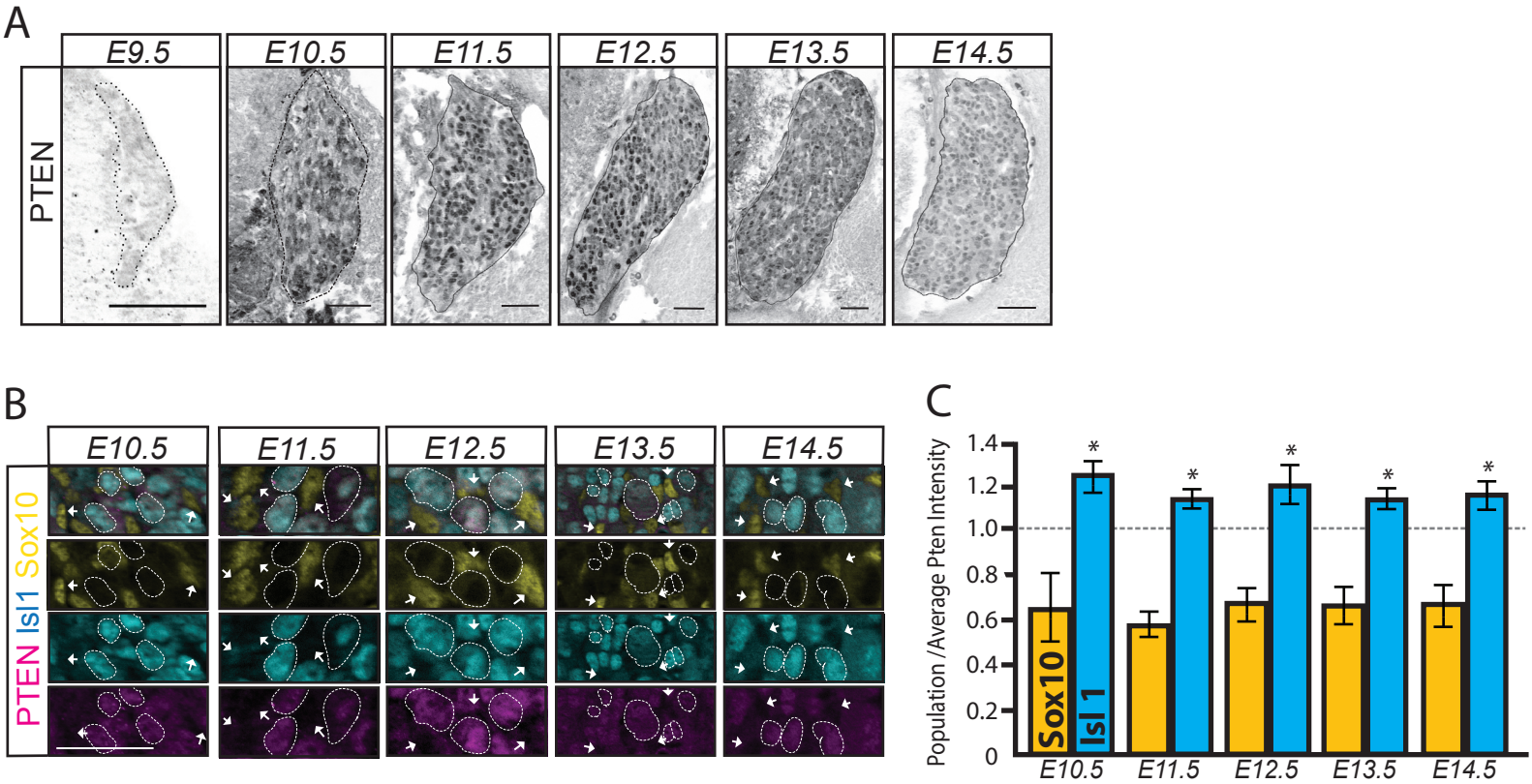
A
E9.5
E10.5
E11.5
E12.5
E13.5
E14.5
PTEN
B
E10.5
E11.5
E12.5
E13.5
E14.5
PTEN Isl1 Sox10
C
Population /Average Pten Intensity
1.4
1.2
1.0
0.8
0.6
0.4
0.2
0
Sox10
Isl 1
E10.5
E11.5
E12.5
E13.5
E14.5

Figure 3

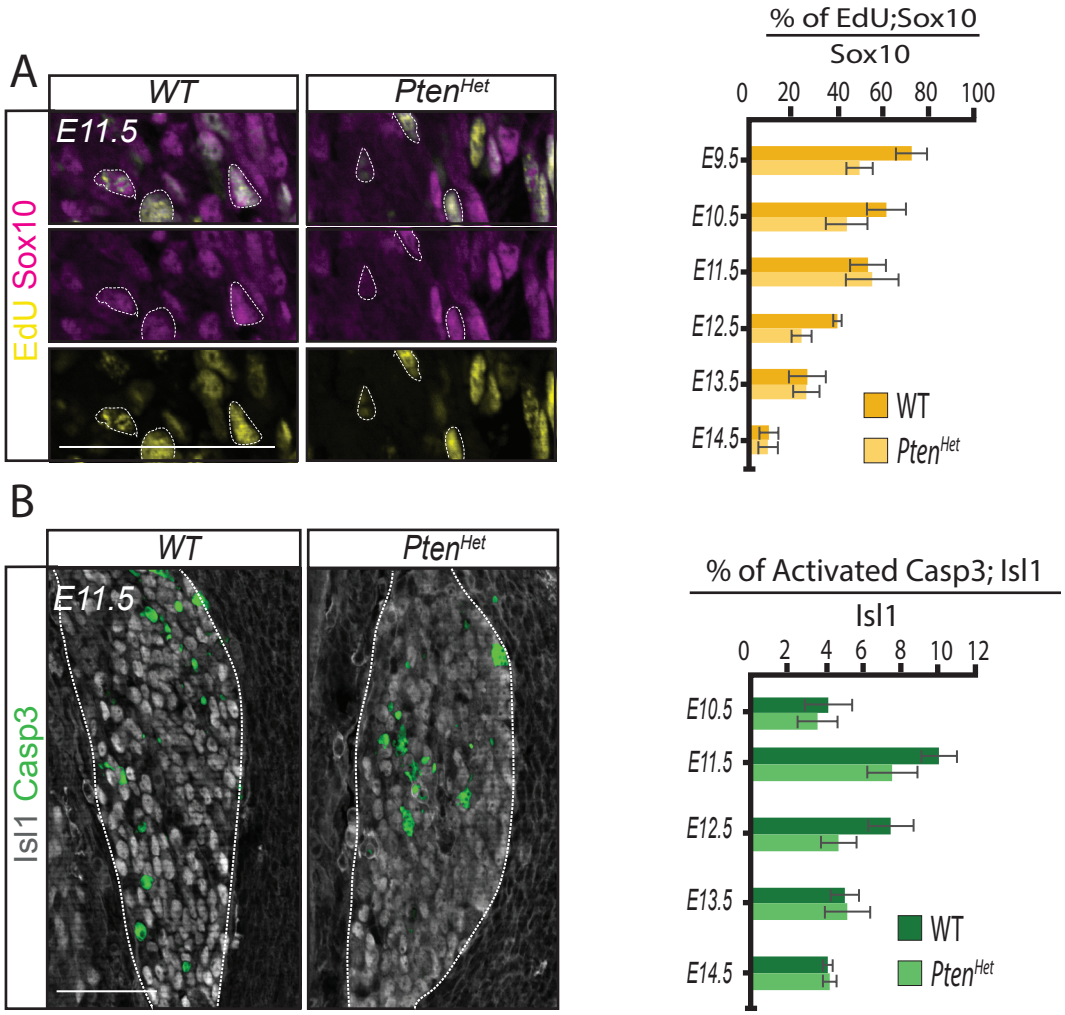
A
WT
Pten^Het
E11.5
EdU Sox10
% of EdU;Sox10
Sox10
0 20 40 60 80 100
E9.5
E10.5
E11.5
E12.5
E13.5
E14.5
WT
Pten^Het
B
WT
Pten^Het
E11.5
Isl1 Casp3
% of Activated Casp3; Isl1
Isl1
0 2 4 6 8 10 12
E10.5
E11.5
E12.5
E13.5
E14.5
WT
Pten^Het

Figure 4

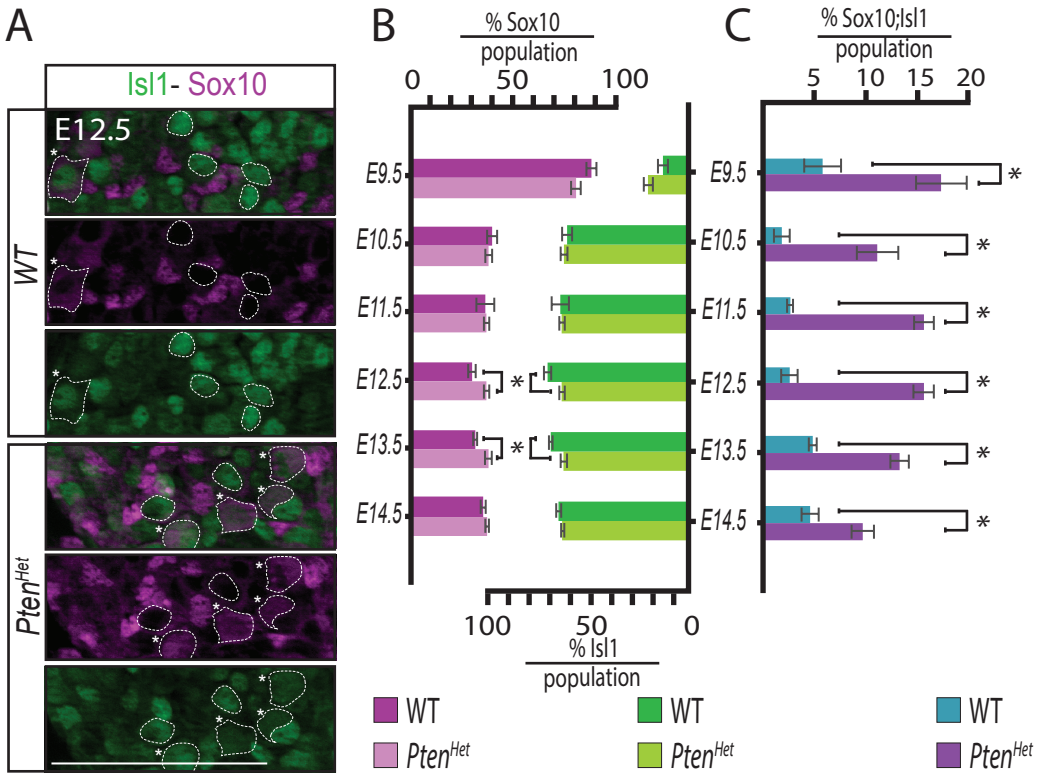
A
Isl1- Sox10
E12.5
WT
Pten^Het
B
% Sox10
population
0
50
100
E9.5
E10.5
E11.5
E12.5
E13.5
E14.5
100
50
0
% Isl1
population
WT
Pten^Het
WT
Pten^Het
C
% Sox10;Isl1
population
5
10
15
20
E9.5
E10.5
E11.5
E12.5
E13.5
E14.5
WT
Pten^Het

Figure 5

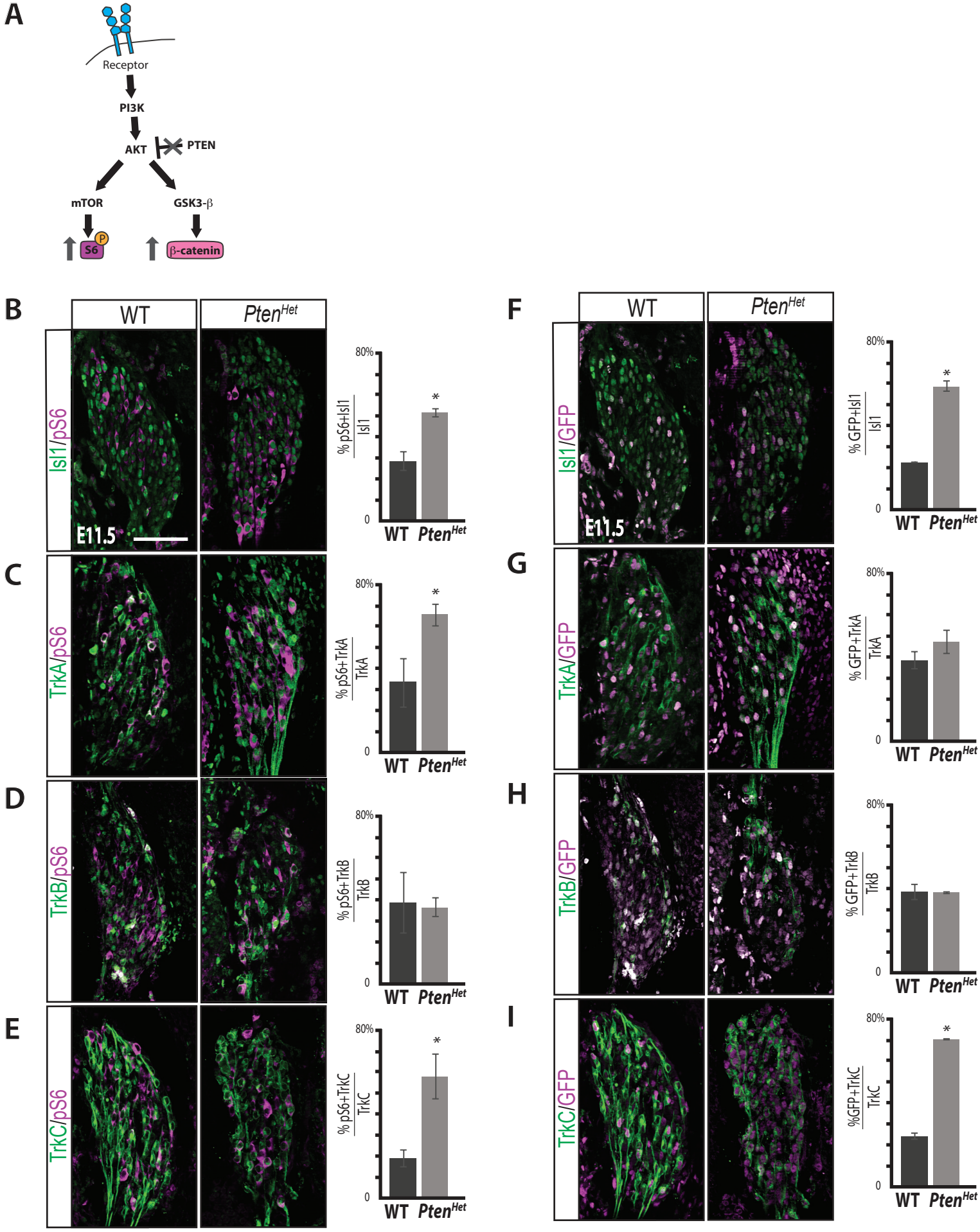
A
Receptor
PI3K
AKT
PTEN
mTOR
GSK3-β
S6
P
β-catenin
B
WT
PtenHet
Isl1/pS6
E11.5
% pS6+Isl1 / Isl1
80%
0
WT
PtenHet
C
TrkA/pS6
% pS6+TrkA / TrkA
D
TrkB/pS6
% pS6+TrkB / TrkB
E
TrkC/pS6
% pS6+TrkC / TrkC
F
Isl1/GFP
% GFP+Isl1 / Isl1
G
TrkA/GFP
% GFP+TrkA / TrkA
H
TrkB/GFP
% GFP+TrkB / TrkB
I
TrkC/GFP
%GFP+TrkC / TrkC

Figure 6

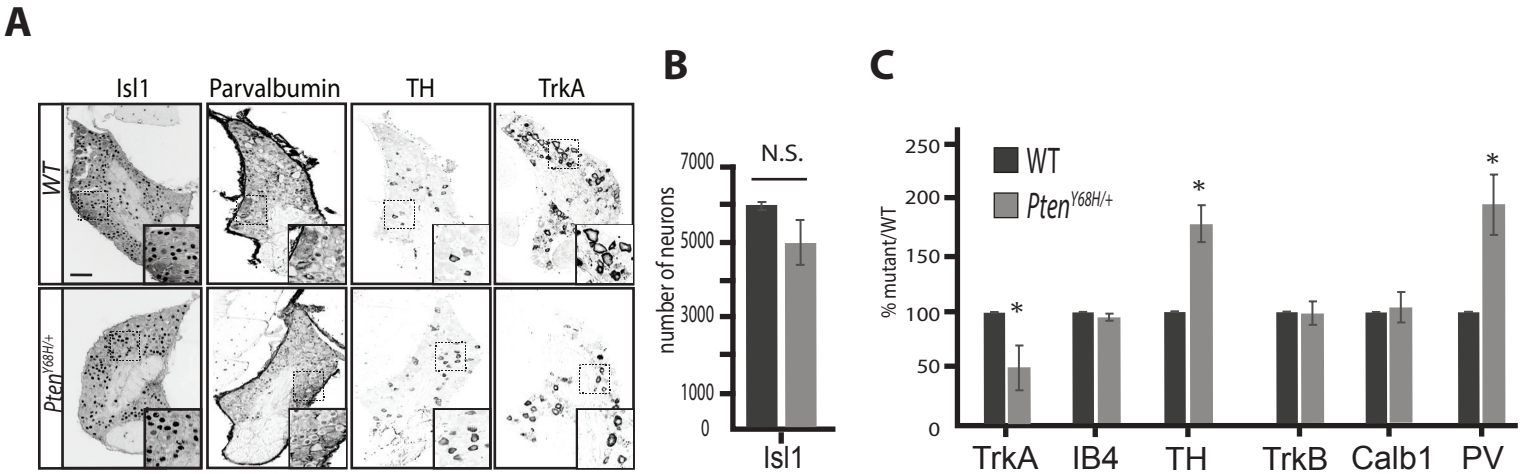
A
Isl1
Parvalbumin
TH
TrkA
WT
Pten Y68H/+
B
N.S.
7000
5000
3000
1000
0
number of neurons
Isl1
C
WT
Pten Y68H/+
250
200
150
100
50
0
% mutant/WT
*
*
*
TrkA
IB4
TH
TrkB
Calb1
PV

Figure 7